The Effects of Media and Platen Design on Pressure in a Thermal Printer Nip

Kenneth D. Stack*, John E. LaFleche and Richard C. Benson

Mechanics of Flexible Structures Project, Department of Mechanical Engineering, The Pennsylvania State University

Charles D. Zinsmeyer

Dimension Mechanical Development, Dell Computer Corporation

The effects of receiver stock and platen covering on pressure in a thermal printer nip were investigated using the nonlinear finite element method. "Design of experiment" techniques were used to reduce computational effort. Pressure in the nip is shown to be dominated by receiver thickness and stiffness. Examples of pressure versus head load are given and the relationship between these important variables discussed.

Journal of Imaging Science and Technology 42: 121–125 (1998)

Introduction

In recent years, thermal printing has become one of the most popular forms of digital imaging. Thermal wax transfer, thermal dye diffusion, and direct thermal printers are used for bar codes, high-end color proofing, and outdoor signs, just to name a few applications. Most of these printers use thermal printheads that contain a small ceramic bead, as shown in Fig. 1. The bead itself is quite small (45 to 60 μm high and about 1.5 mm wide) and contains thousands of tiny resistors (about 100 μm long) used to transfer the wax from the ribbon to the receiver sheet.† The size of the bead shown in Fig. 1 is exaggerated for illustrative purposes only. To enforce intimate contact between the printhead bead, ribbon, receiver, and platen, a vertical load is applied to the printhead. As the pressure beneath the bead increases, thermal contact losses drop off and the result is a print that has a higher optical density.[1] The area of contact between the bead, ribbon, receiver, and platen is known as the "nip region."

One of the design challenges facing thermal printer manufacturers is that customers want to print on a wide variety of receiver papers. These substrates can include calendared paper, vinyl, label stocks, and PVC cards. Because the pressure in the nip region will be a function of the mechanical properties of these materials, different receiver stocks give rise to different optical densities for the same head load. The goal of this study will be to understand how each of the different nip parameters affect the pressure generated beneath the bead.

† Direct thermal printers use receiver sheets that contain a temperature dependent dye and thereby avoid the use of a ribbon altogether.

Original manuscript received March 7, 1997.

* New address Engineering Systems Division, Building 23, Eastman Kodak Company, Rochester, New York 14650

Because the bead itself is so small, directly measuring the pressure would be quite difficult. Common nip widths are very small, on the order of 0.02 to 0.08 mm wide. We will instead use the nonlinear finite element method to model the deformation and contact behavior in the nip. In addition, we will use design of experiment (DOE) techniques[2] to help interpret the data and to reduce our overall computational time.

Past authors have focused on a number of other areas related to thermal printing. Benson et al.[3] and Chiu et al.[4] focused on wrinkling in thermal printer ribbons, a common design issue. LaFleche et al[5] and Kaneko[6,7] studied the dye-transfer process while Sentani[8] focused on temperature modeling of the head. Stack et al.[9] and Diehl et al.[10] used nonlinear finite elements to model nip mechanics problems related to photocopying.

Finite Element Model

Figure 2 shows a finite element model of the thermal printer nip. The simulations in this study were performed using the ABAQUS nonlinear finite element program.[11] The curved, thin line at the top represents the thermal printhead bead, which we assume is rigid. The receiver paper and

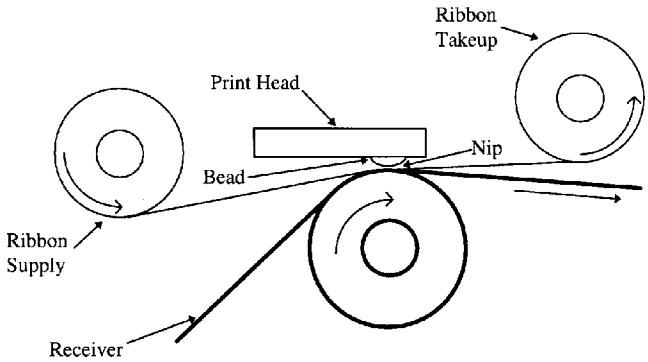

Figure 1. Thermal printer schematic.

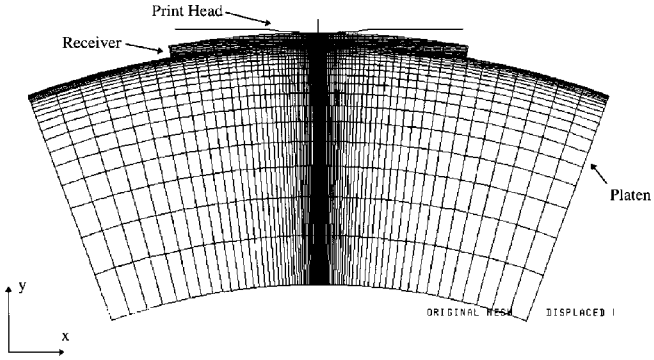

Figure 2. FEA model.

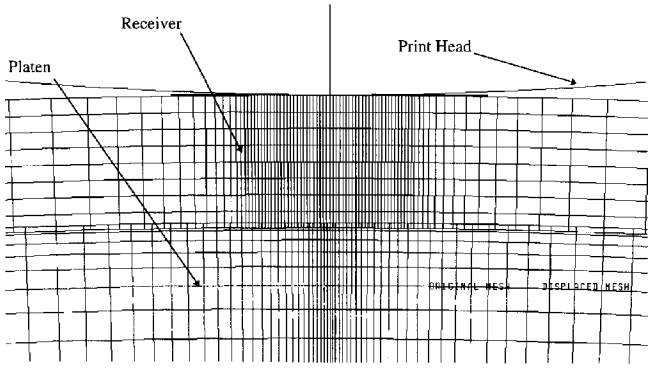

Figure 3. Close up of nip region.

platen are modeled using 4 noded, plane strain, reduced integration elements. We only need to model a total of 40 deg of the platen and 20 deg of the receiver to model the pressure distribution accurately. Far away from the contact region, the stresses and deflections are quite small and, therefore, these portions of the mesh can be neglected.† Also note that we have neglected the ribbon in this model. The ribbon is so thin (4 to 6 μm) it adds little in terms of mechanical response. Figure 3 shows a close-up view of the nip region. We have used a denser mesh to predict the contact behavior in this region accurately. The model also assumes that the platen roller core is rigid and that the printhead bead itself has no variation across the nip.

We do not know, a priori, the size of the contact regions between the printhead and receiver or the receiver and the platen. We will solve for these contact regions iteratively, using contact elements. ABAQUS checks to ensure that, for example, the printhead does not pass through the surface of the receiver. If it does, the nodes on the receiver are forced to lie along the printhead surface through the use of Lagrange multipliers. The location of each of these nodes along the surface is solved iteratively by a Newton-Raphson technique. See the *ABAQUS Theory Manual*[11] for more details on the solution of contact problems using nonlinear finite element techniques. The displacements of the receiver and platen are solved using standard nonlinear finite element techniques.[11] For the head loads considered in this study, deformations were sufficiently small such that a small displacement strain formulation could be used.

Designed Experiment

Design of experiments (DOE) techniques are used in a variety of applications and industries to understand and interpret the results of experiments. In addition, DOE allows the investigator to significantly reduce the total number of experiments needed. A variety of references exist on DOE techniques[2] and the unfamiliar reader is encouraged to review this material. While most investigators use these methods with laboratory experiments, DOE techniques are also applicable to computer modeling. We will use DOE techniques to analyze the results of our finite element model and reduce the total amount of computation.

TABLE I. Variable Ranges

Factor	Level 1	Level 2	Level 3
Platen Thick	2.54 mm (0.1 in)	7.52 mm (0.3 in)	5.08 mm (0.2 in)
Platen Stiff.	1.03 Mpa(150 psi)	2.07 Mpa(300 psi)	3.1 Mpa,(450 psi)
Rec. Thick.	0.0762 mm(0.003 in)	0.127 mm (0.005 in)	0.178 mm (0.007 in)
Rec. Stiff	1.03 Gpa(150 kpsi)	2.07 Gpa(300 kpsi)	3.1 Gpa(450 kpsi)

TABLE II. Orthogonal Array

Exp. #	Platen Thick.	Platen Stiff.	Rec. Thick.	Rec. Stiff.
1	1	1	1	1
2	1	2	2	2
3	1	3	3	3
4	2	1	2	3
5	2	2	3	1
6	2	3	1	2
7	3	1	3	2
8	3	2	1	3
9	3	3	2	1

Table I shows the factor ranges we will use in our experiments. These ranges were chosen based upon the receiver stocks and platens used in actual thermal printers. Thermal printers normally use elastomeric platen coverings (usually polyurethane, neoprene, or silicon rubber) that have durometers that range from 40 to 80 Shore A. Durometer does not have a direct correlation to elastic modulus, so we have performed compression tests of platen materials to determine the range given in Table I. With one of the advantages of thermal printing being that it can be used on a variety of receiver materials, receiver thicknesses and stiffness can vary quite a bit. The ranges shown for receiver thicknesses and stiffnesses are typical of that which some printers are forced to contend.

Table II shows the orthogonal array of experiments we used in our study. This in known as an L_9 (Phadke[2]) array, and it contains the minimum number of experiments needed to determine the relative importance of each factor. The orthogonal array tells us exactly which levels of each factor must be tested against one another to extract the most information possible while doing the least number of experiments. Each factor can be adjusted to three different levels. If we were to perform enough experiments so that we test each variable at each different level (full factorial of experiments) we would need 81 different test cases. Instead, the use of the orthogonal array allows us to perform only 9 experiments and still compare and contrast the different variables. What we give up by using this orthogonal array is the interactions between variables. Higher order orthogonal arrays can be used to account for some of the interactions, but for our purposes they are not necessary.

Pressure and Deflections in the Nip

The first example we discuss is for the nip parameters (platen-covering thickness and stiffness and receiver thickness and stiffness) set to their mid-range values from Table I. This example is meant to represent a common

† A number of mesh density and mesh size studies were run to confirm our assumption.

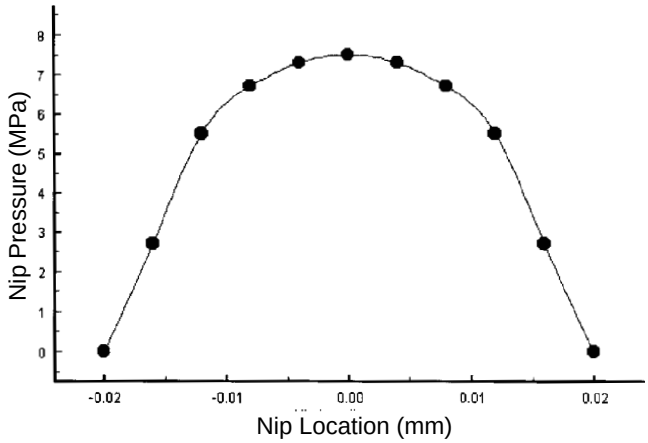

Figure 4. Nip pressure distribution for 0.22 N/mm head load.

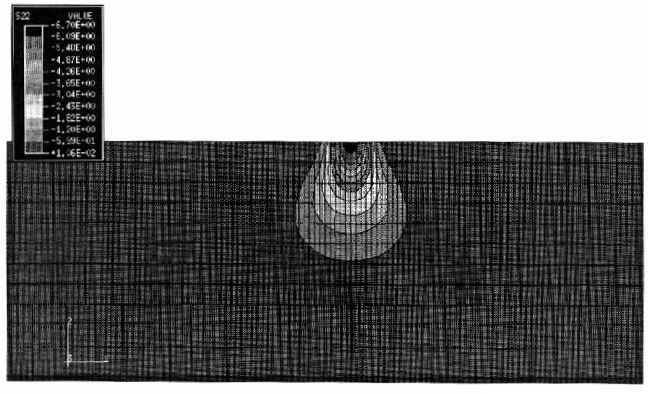

Figure 5. Y direction stress contour in receiver and platen.

configuration. The next section details an investigation into the effects of the various parameters. The maximum head load in this case will be 0.22 N/mm (1.2 lb/in.^{2}), and the platen core will be assumed rigid. The friction coefficients at the printhead/receiver interface and receiver/platen interface were 1.0 and 0.1, respectively. The Poisson's ratio for the platen material was 0.475 and 0.3 for the receiver materials and the outer radius of the platen core was 6.35 mm (0.25 in.).

Figure 4 shows the pressure in the nip region for a head load of 0.22 N/mm (1.2 lb/in.^{2}). It is Hertzian[12] in nature, with the highest pressure being in the center and dropping off toward the edge. Notice that the nip width, even at this head load, is only about 0.04 mm, which is less than the length of the resistive element itself. This small nip width is why so much care must be taken when aligning the printhead to the platen. Figure 5 shows the pressure contours in the receiver and platen covering. Note that the stress in the receiver is very localized. The stresses in the platen layer are quite small, which is why we only need to model 40 deg of the roller.

It is often asked whether the Hertz contact solution can be used to approximate the pressure and nip width for a given head load. The Hertz solution is available in most engineering mechanical design textbooks.[12] Hertz's theory was developed for the contact of two dissimilar cylindrical bodies. Our case has three different entities, the printhead, receiver, and platen. If we assume that the receiver is thick enough so that it acts like an infinite half-space, then we can compute the Hertz contact solution. This assumption is often used in problems involving thermal printers, but for many cases it does not accurately model the nip behavior. The print head is again assumed rigid, just like our finite element model. From Shigley,[12] the nip width is given by

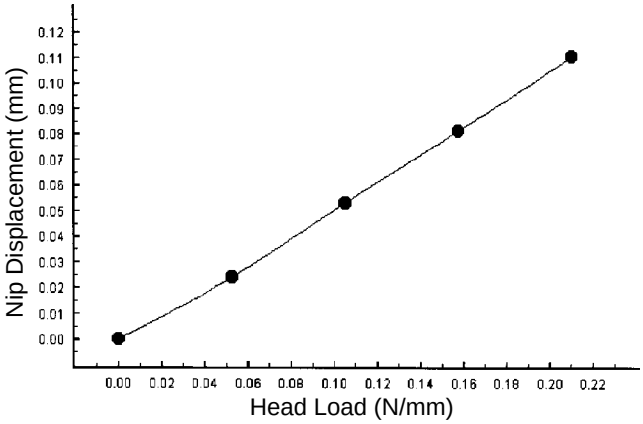

Figure 6. Head indentation versus head load.

$$\text{nipwidth} = 2\sqrt{2\frac{F}{\pi}\frac{(1-\upsilon^2)}{Er}\left[\frac{1}{\frac{1}{2Rr}+\frac{1}{2Rh}}\right]}, \qquad (1)$$

where F is the head load per unit depth, ν is Poisson's ratio, E_r is the modulus of the receiver stock, R_r is the outer radius of the receiver, and R_h is the radius of the printhead bead. The maximum pressure in the nip is given by

$$P\max = \frac{4F}{\pi \cdot \text{nipwidth}}. \qquad (2)$$

For the values used in this example, that would give a maximum pressure of 10 MPa and a nip width of 0.028 mm. That overestimates the pressure and underestimates the nip width by about 40%. If the receiver stock was very stiff and thick, then indeed the Hertz approximation may hold true. This may be applicable to PVC card stocks and other specialty receivers. For most labels stocks and papers, however, the Hertz contact approximation is not appropriate.

Figure 6 shows the indentation of the printhead bead as a function of head load. The response is very linear for this set of nip parameters. The total amount of displacement is only 0.12 mm (0.0047 in.) for our maximum head load of 0.22 N/mm (1.2 lb/in.^{2}). This small amount of displacement causes many difficulties in printer design. Even a small change in the relative thickness of receiver stock or platen thickness will lead to large changes in the resulting pressure underneath the head. This causes printer manufacturers to make platens and heads with very tight tolerances on smoothness and thickness. Figure 7 shows the peak pressure in the nip as a function of head load. Pressure increases quickly but then reaches a point of "diminishing return." The shape of this curve is determined by both the amount of indentation of the bead and the relative radii of the printhead bead and receiver/platen combination. The shape of this curve is also characteristic of the optical density as a function of head load. See Ref. 1.

The Relationship Between Head Load and Nip Pressure

Our first objective is to determine the factors that govern peak pressure in the nip. We have run the experiments

TABLE III. Results for Experiments 1 through 9

Exp. #	P_{max} (MPa)	S/N ratio
1	1.8	5.1
2	8	18.1
3	15	23.5
4	9.5	19.6
5	4.2	12.5
6	4.5	13.1
7	8	18.1
8	7.5	17.5
9	3.6	11.1

TABLE IV. ANOM Table for Maximum Nip Pressure

Factor Level	Platen Thickness	Platen Stiffness	Receiver Thickness	Receiver Stiffness
Level 1	15.6	14.2	11.9	9.5
Level 2	15.0	16.0	16.2	16.4
Level 3	15.6	15.9	18.0	20.2

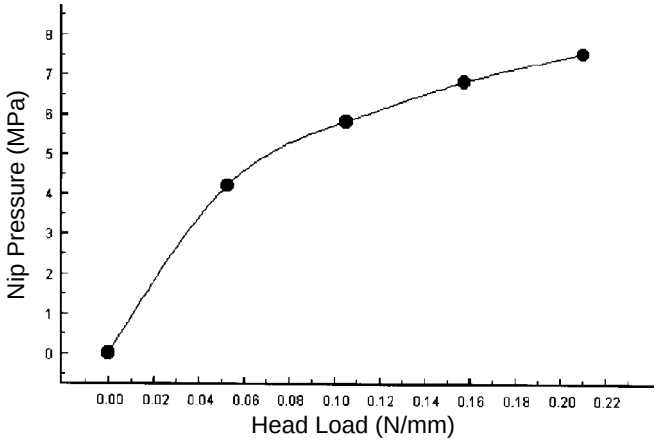

Figure 7. Peak nip pressure versus head load.

outlined in Table II using our finite element model. These simulations used a maximum head load of 0.22 N/mm (1.2 lb.in.^{2}) and the circular printhead bead was 60 μm high and 1.15 mm wide. To demonstrate the differences between the tests, Fig. 8 shows the maximum pressure in the nip versus head load for Experiments 1, 2, and 3. We see that by changing just a few of the parameters the resulting nip pressure is quite different for each case. Experiment 1 had all of the variables set at their lowest possible settings. This is the softest, thinnest receiver on top of the softest, thinnest platen covering. We see that the pressure first increases then begins to decrease! The other two experiments, where the receiver and platen are somewhat stiffer, exhibit more intuitive behavior. As head load rises head pressure beneath the bead increases as well.

The explanation for Experiment 1 is important because many thermal printer manufacturers see this behavior in the form of an optical density drop after a certain head load is reached. To illustrate this behavior, we will look at the nip pressure distribution. Figure 9 shows the pressure distribution in the nip at a head load of 0.09 N/mm. The pressure distribution is Hertzian in nature, similar to that of Fig. 4. We would expect that as we increase head load, the pressure would increase as well. Figure 10 shows the pressure distribution at a head load of 0.18 N/mm (1 lb/in.^{2}). We see that not only is the distribution different, but the peak pressure has actually dropped. This unusual change in nip

TABLE V. ANOVA Table for Maximum Nip Pressure

Factor	DOF	Sum of Squares	Mean Square	*F*	% Var.
Platen Thick.	2	0.6	0.3	0.1	0.2
Platen Stiff.	2	5.9	2.9	1.0	2.5
Rec. Thick.	2	59.6	29.8	9.9	24.8
Rec. Stiff.	2	174	87.0	29.0	72.5

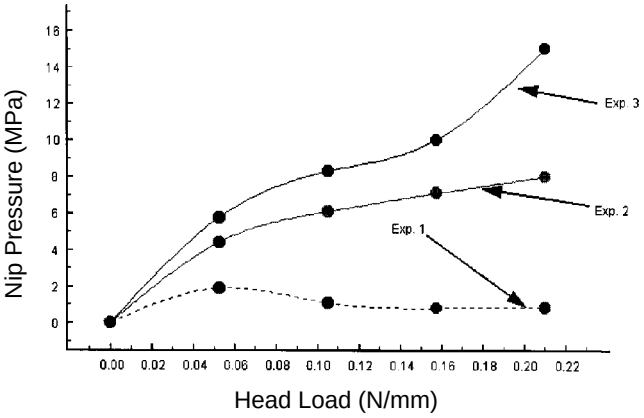

Figure 8. Peak nip pressure versus head load for Exp. 1 through 3.

pressure is caused by the receiver paper acting like a beam on an elastic foundation, a problem considered in many materials strength textbooks.[13] The combination of receiver thickness and stiffness, platen thickness and stiffness, friction, and geometry leads to this behavior and is generally a problem only for thin, soft receivers.

To the printer designer this means that for some combinations of receiver and platen covering, they run the risk of obtaining decreased nip pressure at higher head loads. Notice also that the peak pressure in Fig. 10 is not underneath the resistor, but rather farther out at the edges of the nip. Because we are using pressure to reduce thermal contact losses in the nip, we would like the pressure to be at a maximum underneath the resistor itself. The authors hope to address this behavior in more detail during future research.

Factors That Determine Maximum Pressure in the Nip

In Table III, the S/N column was computed using the Taguchi[2] definition of

$$S/N = -10 \log\left(\frac{1}{P\max^2}\right). \quad (3)$$

The appropriateness of using the S/N ratio depends on the multiplicative nature of the factors, and again the reader is referred to Phadke[2] for more information. A simple definition of S/N is that it shows the relative performance of each experiment. Because we are investigating the effects of each parameter on the magnitude of the pressure in the nip, the larger the value of P_{max} the larger the value of the S/N ratio.

To find the levels for each factor that maximize nip pressure, we perform an analysis of the means (ANOM). Simply stated, this involves taking the averaged values of the objective function for each factor at each level and picking the best setting. The mean value of the S/N ratio for all of the experiments was 15.4. The results of the ANOM analysis are summarized in Table IV and Fig. 11. Clearly the factors that have the largest influence over the maximum nip pressure are the receiver thickness and stiffness. The platen thickness and stiffness are small players when compared to the receiver properties. As one would expect, the

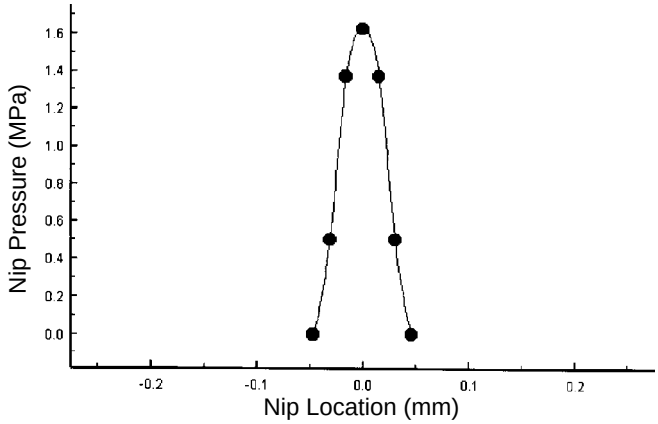

Figure 9. Exp. 1 nip pressure, 0.09 N/mm (0.5 lb/in.) head load

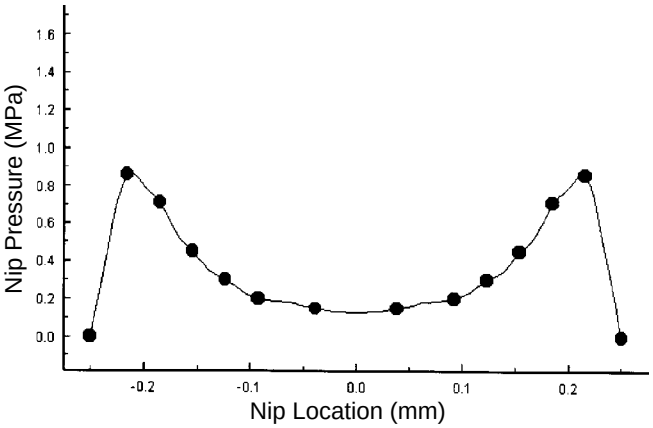

Figure 10. Exp. 1 nip pressure, 0.18 N/mm (1.0 lb/in.) head load.

thicker, stiffer receiver papers will cause higher overall nip pressures.

Additional information can sometimes be gleaned from analysis of the variance of the means (ANOVA). For our case, we can clearly see the results from the ANOM, but the ANOVA results are given in Table V, for completeness. See Phadke[2] for more information on ANOVA analyses. The last column, percent variance, gives us the relative performance of the given factors. The percent variance is the percentage of variance from the mean value of the S/N for each factor. The bigger the variance, the more response of the given factor. In our case, the receiver stiffness accounts for 72% of the maximum pressure. The receiver stiffness follows with 25%, and the platen thickness and stiffness account for almost none of the variance.

Conclusions

The design conclusion from the DOE is that the receiver stiffness and thickness dominate the behavior in the nip. This is an unfortunate result from a design point of view. The printer manufacturer often has control only over the platen thickness and stiffness. The customer has control over the receiver stock he or she wishes to use. This means that the manufacturer cannot control the nip pressure if the customer uses a variety of receiver papers. This is often the case for thermal printers and represents one of the most difficult design challenges facing printer engineers. Because the nip pressure can change so much from receiver type to receiver type, the optimum head load to provide the highest optical density will also change from receiver stock to receiver stock. Sometimes, the only fix is to make the head load adjustable based on the receiver

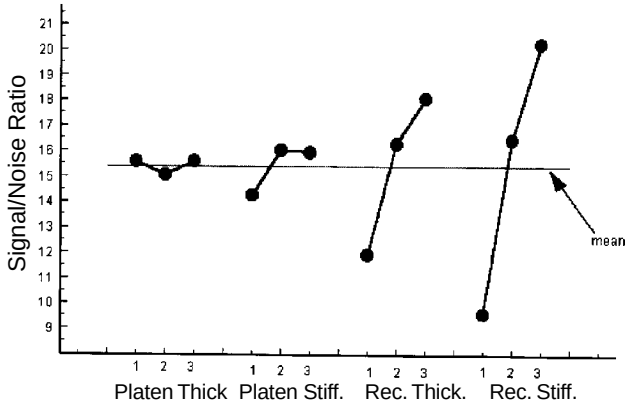

Figure 11. ANOM results for maximum nip pressure.

type. This is often not a simple task and is highly undesirable from an ease-of-use perspective.

For thin, soft receiver stocks in combination with soft platen coverings, the nip pressure may not always rise as head load is increased. A "snap through" effect can be seen, and the pressure distribution under the print head bead can become quite unusual. This effect can be avoided through the proper combination of platen stiffness and receiver stock and is seen only when printing on thinner substrates.

The results in this study assumed that the platen core and the print head were stiff and that no bending took place in either part. Future work will investigate the effects of bending in the nip and the subsequent axial variation in pressure and nip width. One can imagine that any axial variation in pressure will lead not only to optical density variations across the printer, but can cause ribbon wrinkling and receiver misregistration as well. This study however forms the basis for the behavior of the thermal printer nip and shows that the nonlinear finite element method can be used to model the mechanics of the nip region.

Acknowledgments. The authors wish to thank the Summagraphics Corporation for supporting the initial development of the finite element model. We would also like to thank Dr. Ted Diehl of the Motorola Corporation for his insightful comments and suggestions.

References

1. K. Hanma, "A color video printer with sublimation dye transfer method," *IEEE Trans. Consumer Electron.* **CE-31** (3), 431 (1985).
2. M. Phadke, *Quality Engineering Using Robust Design*, Vol. 1, Prentice Hall, NJ,1989 .
3. R. Benson, H. Chiu, J. LaFleche, and K. Stack, "Simulation of wrinkling patterns in webs due to non-uniform transport conditions," in *Proc. 2nd Annual Conf. Web Handling*, OSU, 1993, p. 333.
4. H. Chiu, R. Benson and S. Burns, "Thermal and mechanical wrinkling of polymer membranes," in *AMD* **149**, *Web Handling,* ASME 1992, p. 49.
5. J. LaFleche, R. Benson, K. Stack, and S. Burns, "Thermal dye diffusion printing," in *ISPS Proc.* ASME 1996, p. 21.
6. A. Kaneko, "A simple simulation for simultaneous diffusion of dye and heat in dye diffusion thermal transfer printing Part I: Evaluation," *J. Imaging Sci.* **35**, 49 (1991).
7. A. Kaneko, "A simple simulation for simultaneous diffusion of dye and heat in dye diffusion thermal transfer printing Part II: Application", *J. Imaging Sci.* **35**, 263 (1991).
8. K. Setani, "Thermal control method for sublimation type thermal dye transfer printing," in *Proc. SPIE* **1252**, 144 (1990).
9. K. Stack, T. Diehl, and R. Benson, "A plane strain nonlinear finite element model for nip mechanics," *Comput. Structures*, (submitted).
10. T. Diehl, K. Stack, and R. Benson, "A study of three dimensional nonlinear nip mechanics," in *Proc. 2nd Annual Conf. Web Handling*, OSU 1993, p. 161.
11. Hibbitt, *ABAQUS Theory Manual*, HKS Inc., RI, 1996, Sect. : 5.1.3.1.
12. Shigley, *Mechanical Engineering Design*, McGraw-Hill, New York, 1989, p. 71.
13. Timoshenko, *Plates and Shells*, McGraw-Hill, New York, 1959, p. 30.